Indian Journal of Engineering & Materials Sciences
Vol. 29, December 2022, pp. 744-749
DOI: 10.56042/ijems.v29i6.70275

# Experimental and Finite Element Studies of Stretch Forming Process for ASS 316L at Elevated Temperature

Baloji Dharavath[a]*, M T Naik[b], Anand Badrish[c], Tanya Buddi[d], & Kuldeep K Saxena[e]

[a] Department of Mechanical Engineering, KG Reddy College of Engineering & Technology, Hyderabad 500 075, India
[b] Department of Mechanical Engineering, JNTUH, Hyderabad 500 072, India
[c] D.O.F.S, DRDL, Hyderabad 500 058, India
[d] Department of Mechanical Engineering, GRIET, Hyderabad 500 090, India
[e] Department of Mechanical Engineering, GLA University, Mathura 281 406, India

*Received: 9 September 2022; Accepted: 17 October 2022*

Austenitic stainless steel 316 L grade is a material having extraordinary mechanical properties, low cost and easily available. This is the reason it was used in various industrial and nuclear applications. In the present work, ASS 316L nakazima specimens are stretched under hot forming conditions (750°C, 825°C and 900°C) at a constant strain rate (0.1s-1) along with three different orientations. These six types of nakazima specimens were used to know the formability behaviour of the material with the help of forming limit diagrams (FLD) obtained by the stretch forming process. A smaller change in Punch load and an increase in displacement were observed, which indicates the formability improvement of ASS 316L sheet metal with the increase in temperature. In addition, ABAQUS 6.13 computer code was applied for the prediction of formability from 750°C to 900°C. To improve the accuracy of the simulation, a number of integration points were accrued within the thickness direction, limiting dome height (LDH).The ductile fracture was observed from SEM images for all the temperatures. A close agreement was found between experimental and simulated results.

**Keywords**: Austenitic stainless steel 316L, Stretching, Hot forming, Forming limit diagram, Limiting dome height, Finite element analysis

## 1 Introduction

Austenitic stainless steel 316L materials are used for various critical applications in nuclear industries like high temperature and high-pressure operating conditions. Fuel rod cladding in nuclear reactor and also heat exchanger body parts uses this ASS grade material because of their extraordinary mechanical properties. The formability and ductility improved at elevated temperatures compared with room temperature [1-6].

Hot forming is a process for plastically deforming the material above recrystallization temperature. It is simple to make high strength material into useful products. ASS 316L material also having its high-temperature applications in various industries. particularly at elevated temperatures flow stress decreases in the material. The mechanical properties are optimised to evaluate the effective characteristics by Response Surface Methodology. Forming at room temperature is a big problem for shaping high strength and hard materials into sheets into useful products [7,8].

The strain rate is one of the most affecting parameters on the formability of ASS 316L and forming strains are also determined at various elevated temperatures and lower strain rates, The ductility and formability increase.[9,10] Hot forming is the only way to solve these problems at room temperature for ASS materials. Formability at high temperatures improves the production rate and it was more effective in industries[11-16]. The corrosion resistance of this material is more because of 2-3% molybdenum, due to this property it was used in various shipbuilding applications. The sub-zero mechanical properties like ultimate tensile strength, yield strength and % elongation areoptimised by using Taguchi robust design. The strength of the material improved at sub-zero temperatures and ductility decreased, because of this reason it was used as liquid nitrogen gas cylinders[17]. One of the other element reasons for the non-corrosive properties towards oxygen is chromium. This element will protect the

*Correspondence author
(E-mail: baloji.dharavath333@gmail.com)

steel by forming a thin layer of chromium oxide on the surface of the ASS316 L sheet to resist the corrosion effects[18].

A standout amongst other options is the Finite Element Analysis of the stretch-forming process. FE simulations generally rely upon the material models utilized and the accuracy of the input material information. Chiefly, the determination of a suitable yield model is fundamental since it gives an accurate prediction of the noticed starting and ensuing yield behaviours of a material[19]. To arrive at the optimum set of method parameters, traders practice trial and error methodology. A quality product requires an incredibly tedious and long process to reach an optimum setting. To reduce the product's price and improve its quality, it is imperative that experiments are designed so that selected method parameters can be improved. Assorted parameters were tested on the deep drawing of AA7075 and the results were eventually supported by finite element analysis (FEA)[20]. Complete formability information of metal can be gathered from the FLD. High formability is expected in metals having distributed strains below FLC. Various strain conditions can be easily evaluated in the same FLD plot and fracture limit can also be evaluated for a particular combination of strains[21] .

Some investigations were carried out on different ASS grade materials, Swadesh et al. studied the formability characterization of ASS 304,316,316L grades at warm forming and reported that improved formability and ductility and also simulated by using LS-DYNA software[22,23]. In this present investigation stretching operations and simulations were carried out on different sizes of nakazima samples at elevated temperatures.

## 2 Materials and Methods

The stretching operation was conducted on an ASS 316L steel sheet of 0.6 mm thick and prepared as six different sizes of blanks (Nakajima) by using a wire-cut EDM process. These blanks are cut according to three orientations (0°, 45° & 90°). The main chemical compositions are carbon 0.03%, silicon 0.19%, Manganese 1.4%, Phosphors 0.034%, Sulphur 0.005% Nickel 10.27% chromium 16.4 % molybdenum 2.08 % and the majority of iron.

The schematic view of stretching process and sample preparation shown in Fig. 1. The present study on ASS 316L sheet and the stretching experiments conducted on a universal testing machine connected

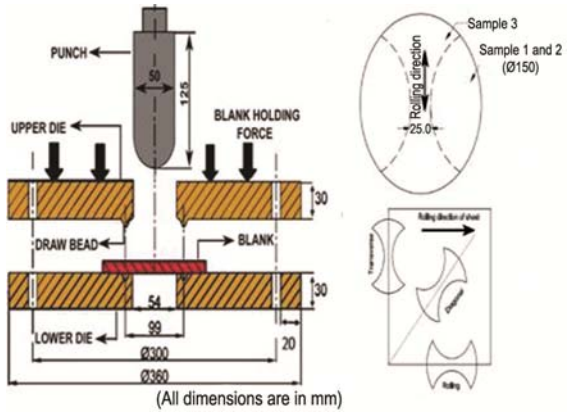


Fig. 1 — Schematic view of Punch and die assembly, preparation of different size of samples and Direction of sampleto the rolled sheet (RD, TD, DD).

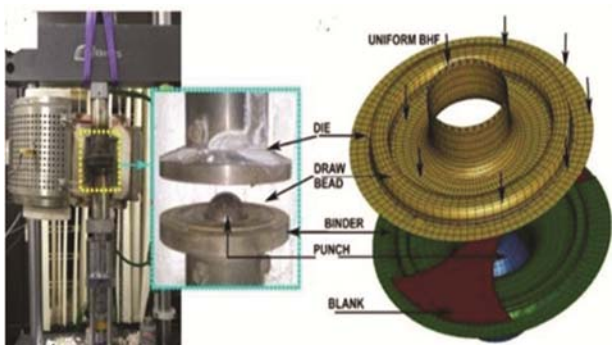


Fig. 2 — Metal hot Forming setup with heating furnace.

with a heat furnace capacity of $900^0$C shown in Fig. 2. In this investigation, nakazima samples stretched up to fracture point at hot forming conditions and those fracture strain values were used for forming limit diagrams. The process parameters are affected; blank materials are strain rate, blank holding force.

The nakazima specimens were prepared three orientation wise (rolling, transverse and diagonal) with the help of wire-cut EDM process. Figure 3(a) shows six types of nakazima samples before testing, which were stretched at 0.1/s strain rate and elevated temperatures. The 50 mm diameter of punch and blank holding force is required to overcome the defects in the stretching process. One set of stretched samples at 750°C with 0.1/s is shown in Fig. 3(b).

## 3 Results and Discussions

### 3.1 Finite element analysis (FEA)

ABAQUS 6.13 software system was used to simulate the stretching process using a flat bottom punch. Solidworks-14 has been used for the CAD model. The CAD file of the stretch forming process

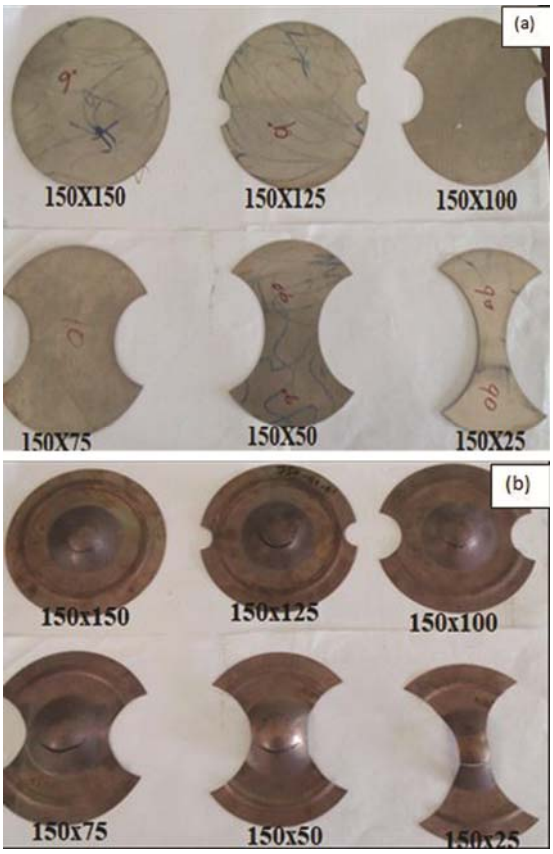


Fig. 3 — (a) Samples with six different sizes before stretching, and (b) After stretching at 750°C with 0.1/s.

accommodates four completely different elements, namely the blank holder, the die, the punch, and the blank as shown in Fig. 4(a). Since no explicit results or observations are required to be done on the punch, die and blank holder, they are specified with distinct fixed properties. For these mesh elements, ABAQUS uses the sort R3D4. A deformable-body property is allotted and solid C3D8R parts are used to enable all the observations to be completed over blanks. It is assumed that the friction coefficient between all components is 0.12. Figure 4(b) represents the simulation run at 900°C for the stretching process.

### 3.2 Punch load and displacement in the blank

The stretching on ASS 316L blanks with six different sizes of (nakazima specimens) done at hot forming conditions. The Fig. 5 (a) demonstrates how to punch load changes with displacement. In most cases, it has been observed that as the temperature increases, the load requirements decrease. Figure 5 (b) presents the load Vs displacement graph for sample design-1. Increasing the temperature causes the punch

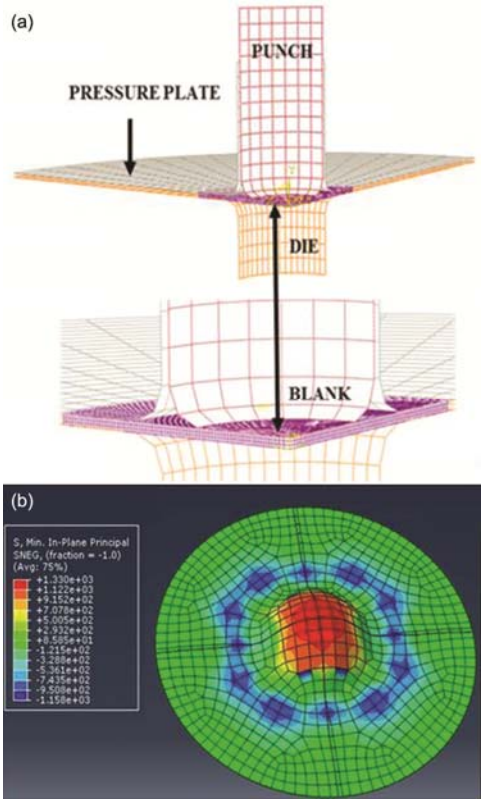


Fig. 4 — (a) Discretization of tools for the stretching in ABAQUS, and (b) Simulation for 150mm blank at 900 °C

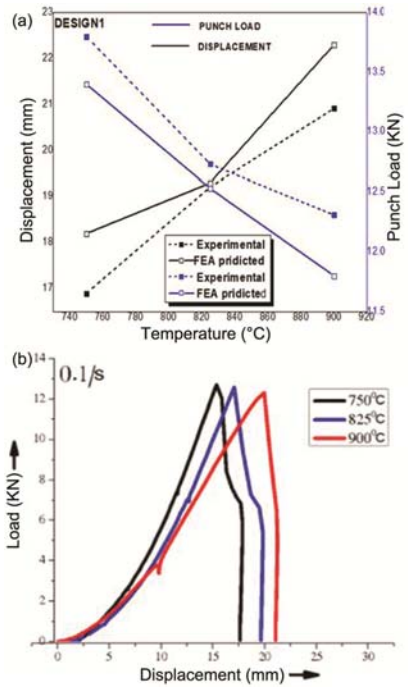


Fig. 5 — Displacement Vs load graph of design-1 (a) experimental and predicted values, and (b) experimental values at different temperatures.

load to decrease slightly and the maximum displacement in the blank. There may be higher chances for defects in smaller size blanks during stretching operation, to overcome these problems optimized blank holding force is required. From results, it was clear that to stretch 150 mm ASS 316L blank at 750° C requires about 13.8 KN load, however, to stretch the same blank at $900^0$ C it takes only 12.3 KN of load and for 25mm diameter ASS 316L blanks seems to be 5.7 KN at $750^0$ C it was 5.1 KN for 900° C. At elevated temperatures, the mean flow stresses of material are decreased, and the drawing force is greater with larger blank size i.e for D-1. Due to the appearance of maximum load, the punch corner radius appears to be necked. Mean flow stress falls in most materials as temperature rises. While heating the material reduces its flow stress, which reduces the deformation stress as well as increases the plasticity of the material, which enables safe drawing of the material[23]. The predicted load-displacement values for various elevated temperatures were similar to the experimental values and the relative error for all designs was well within 5% of acceptance.

### 3.3 Experimental and Theoretical Prediction of Hot Forming behaviour

A forming limit diagram (FLD) which includes true major and minor strains at 3 different temperatures is illustrated in Fig. 6(a). A solid line and a dotted line were used in the illustration to aid in simple identification of experimental and predicted values. This line separation of the failure and safe regions in an FLD. FLDs analyze tension-compression (T-C), plane strain and tension-tension (T-T). There was a difference in slope within T-T. and T-C. Within this T-C region, the slope strain paths accumulated and decreased within the T-T region as the process temperature increased. Due to the gradual rise to 900°C in temperature, the forming limiting strain improved by approximately 57%. Material limiting strains are greatly influenced by the forming temperature. The softening of the material occurs as the temperature rises, resulting in an increase in the material's formability. In Fig. 6(a), smaller changes in FLD curves are detected under the same conditions as those observed by Finite Element Analysis. An ASTM E2218-15 standard punch is 101.4 mm in diameter but has been omitted in favor of a hemispherical punch of sub-sized size (50 mm in diameter) to be used for stretch forming. Material

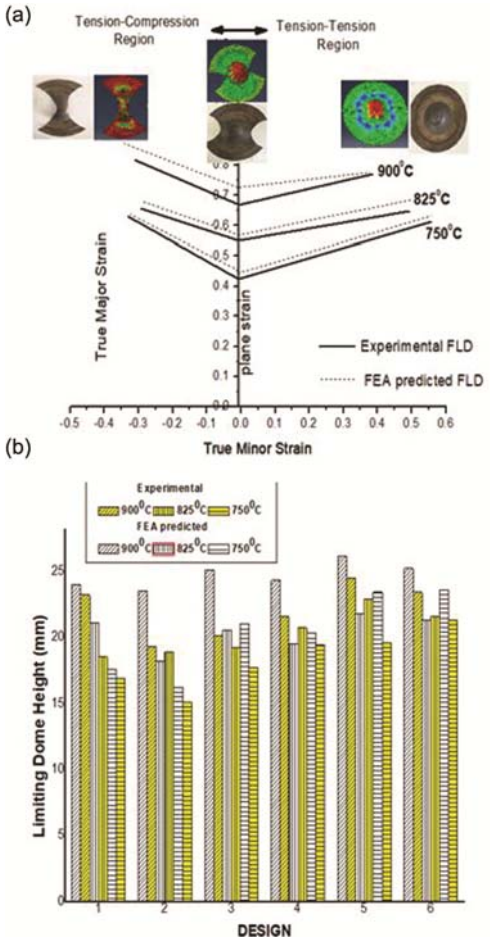


Fig. 6 — Comparison between experimental and predicted graphs for (a) FLD, and (b) LDH.

formability depends largely on the Limiting dome height (LDH) phenomenon. In Figure 6(b), (LDH) is illustrated at various temperatures experimentally and predicted. As the material becomes softer, its formability also increases, which would result in a higher LDH. All designs had a difference between predicted and measured LDH at elevated heat conditions well below 5%.

Measurement of every specimen three times to determine the thickness distribution for designs 1 and 6 have been shown in Fig. 7(a&b). A minimum thickness was observed at a point where the fracture and necking occurred Since the blank thickness of the cup was almost constant near the middle of the specimen at the start. Increasing in thickness, the specimen is pushed toward the flange. A part of the flat flange of the specimen showed a material almost as thick as the sheet. In the current study, different designs were observed to exhibit similar plots at

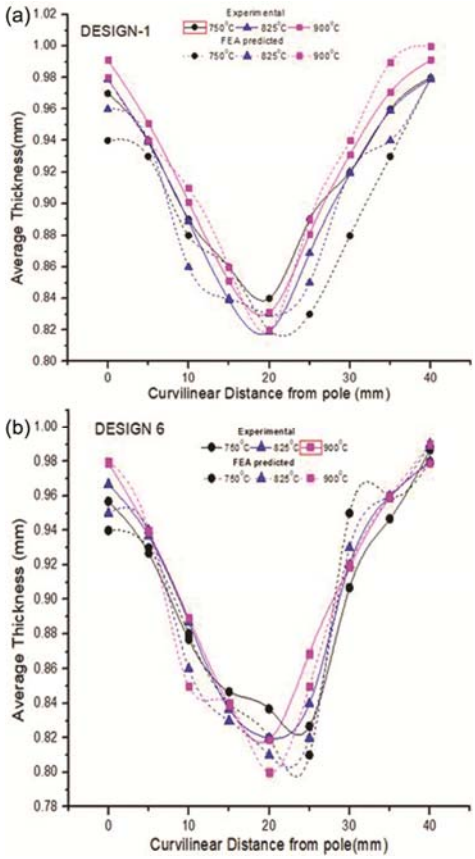


Fig. 7 — Comparison between experimental and predicted thickness distribution for (a) Design-1, and (b) Design-6.

different temperatures. With increasing temperature, there was a decrease in thickness of the necking because the material softens, resulting in increased drawability[16]. A similar curve is also shown by FEA results. In the FEA and experimental results for two different samples of design 1, the thinnest value was found at a pole distance close to 20 mm for 900°C, 825°C, and 750°C The minimum thickness was 20mm distance from pole observed for 900°C, but 22mm distance was observed in FEA. According to design 6, at 900°C and 825°C, the minimum thickness of the sample occurred at approximately 22mm distance from the pole, whereas at 750°C the minimum thickness occurred at approximately 24 mm distance.

### 3.4 Scanning electron microscope (SEM)

ASS 316L sheet samples at elevated temperatures fail by Ductile Fracture as demonstrated by Fig. 8 (a,b,c) with distinct voids, dimples, and flow lines visible at the fracture surfaces. The characteristics of ASS 316L are increasingly ductile as temperatures

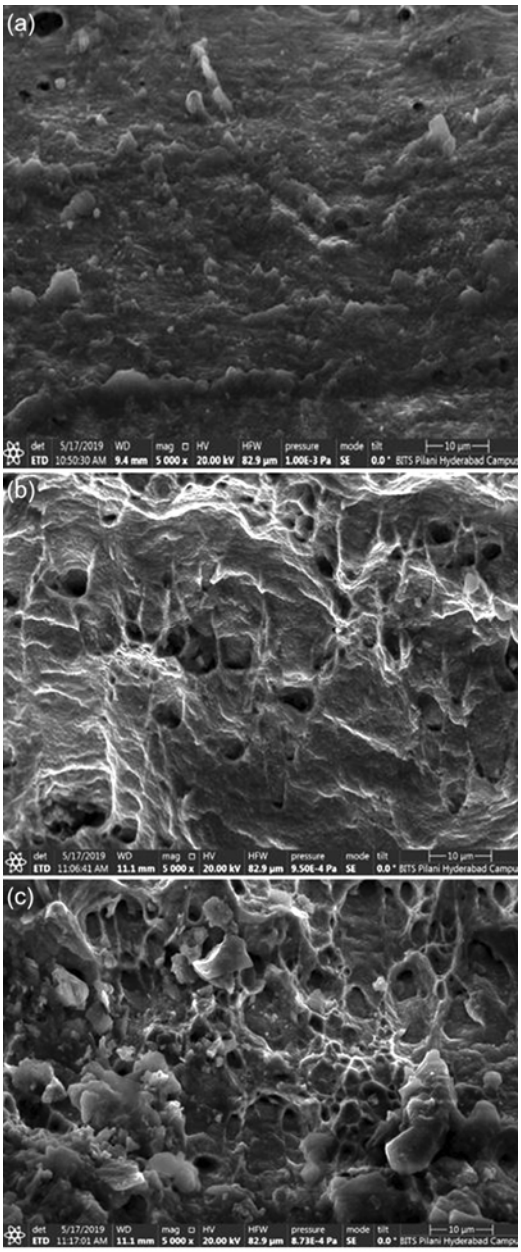


Fig. 8 — SEM (5000X) images of the ASS 316L stretching failure for Design-3 (a) 750°C, (b) 825°C, and (c) 900°C.

rise as a result of the material's increasing flowability. The ductility of the material has improved as the temperature has increased, predominantly due to a reduction in mean flow stress and an improvement in grain boundary movement.

## 4 Conclusion

The material modelling and forming behaviour are mentioned in the current study of ASS 316L. A few important conclusion are listed below

- Forming characteristics of ASS 316L was analyzed based on the stretch forming process. In relation to the limiting strain of the material, the FLDs were compared at varying elevated temperatures. In fact, 57% more forming capability of the material with increasing the forming temperature from 750°C to 900°C, and also this was clear from limiting dome height (LDH) and thickness distribution.
- The fractured part was analyzed by SEM and revealed it to be predominantly ductile at all the temperatures.
- It was found from finite element analysis (FEA) for all designs in the stretch forming process within the acceptance limit.

**Acknowledgement**

It is acknowledged that this work was financially supported by the All-India Council of Technical Education (AICTE) file No: 8-52/RIFD/RPS/ POLICY-1/2016-17 as well as the FIST grant (DST) file No: SR/FST/ College-29/2017 to purchase some special equipment SEM.

**References**

1 Desu RK, Krishnamurthy HN, Balu A, Gupta AK, & Singh S K, *J Mater Res Technol*, (2016) 13.
2 Hussaini SM, Singh SK, & Gupta A K, *Mater Today: Proc*, (2015) 1987.
3 Dharavath B, ulHaq A, Buddi T, Singh SK, & Naik M T, *Adv Mater Proc Technol*, (2020) 384.
4 Gabrera JM, Omar AA, & Prado J M, *J Metall Mater Trans A*, (1997) 2233.
5 Cingara A, & McQueen H J, *J Mater Proc Technol*, (1992) 17.
6 Maheshwari AK, Pathak KK, Ramakrishnan N, & Narayan S P, *J Mater Sci*, (2010) 859.
7 Haq AU, Kavit AK, Rao T, Buddi T, Baloji D, Satyanarayana K, & Singh S K, *Mater Today: Proc*, (2019) 4589.
8 Dharavath B, ulHaq A, Varma MD, Singh SK, & Naik M T, *Mater Today: Proc, 26* (2020) 3179.
9 Badrish A, Morchhale A, Kotkunde N, & Singh S K, *Arab J Sci Eng*, 7 (2020) 45.
10 Gupta AK, Anirudh VK, & Singh S K, *Mater Des*, (2013) 410.
11 Badrish CA, Morchhale A, Kotkunde N, &Singh S K, *Adv Mater Proc Technol*, (2020) 540.
12 Lakshmi A A, Rao C S, & Buddi T, *Mater Today: Proc*, (2019) 2814.
13 Sen N, *Ironmaking & Steelmaking*, (2020) 93.
14 Mahalle G, Morchhale A, Kotkunde N, Gupta AK, Singh SK, & Lin Y C, *J Manuf Processes*, (2020) 482.
15 Sabah S, & Brooks G, *Ironmaking & Steelmaking*, (2016) 473.
16 Pandre S, Morchhale A, Kotkunde N, & Singh SK. *Mater Manuf Processes*, (2020) 901.
17 Baloji D, Anil K, Satyanarayana K, Singh S K, & Naik MT, *Mater Today: Proc*, (2019) 4475.
18 Ramesh R, Dinaharan I, Kumar R, & Akinlabi E T, *J Mater Eng Perform*, (2019) 498.
19 Kotkunde N, Deole AD, Gupta AK, & Singh SK, *Mater Des*, (2014) 336.
20 Venkateswarlu G, Davidson MJ, & Tagore G R, *Int J Eng Sci Technol* 2 (2010) 11.
21 Djavanroodi F, & Derogar A, *Mater Des*, (2010) 4866.
22 Lakshmi AA, Rao C, Kotkunde N, Subbiah R, & Singh SK. Int J Mech Eng Technol, (2018) 403.
23 Singh S K, Mahesh K, Kumar A, & Swathi M, *Mater Des*, (2010) 4478.